Since January 2020 Elsevier has created a COVID-19 resource centre with free information in English and Mandarin on the novel coronavirus COVID-19. The COVID-19 resource centre is hosted on Elsevier Connect, the company's public news and information website.

ARTICLE IN PRESS
+ MODEL
Acta Pharmaceutica Sinica B xxxx;xxx(xxx):xxx

Chinese Pharmaceutical Association
Institute of Materia Medica, Chinese Academy of Medical Sciences

Acta Pharmaceutica Sinica B

www.elsevier.com/locate/apsb
www.sciencedirect.com

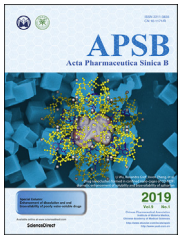

ORIGINAL ARTICLE

Single-shot AAV-vectored vaccine against SARS-CoV-2 with fast and long-lasting immunity

Fuhua Wu[†], Shuang Luo[†], Yongshun Zhang, Yangsen Ou, Hairui Wang, Zhaofei Guo, Chunting He, Shuting Bai, Penghui He, Min Jiang, Xiaoyan Chen, Guangsheng Du, Xun Sun[*]

Key Laboratory of Drug-Targeting and Drug Delivery System of the Education Ministry and Sichuan Province, Sichuan Engineering Laboratory for Plant-Sourced Drug and Sichuan Research Center for Drug Precision Industrial Technology, West China School of Pharmacy, Sichuan University, Chengdu 610041, China

Received 16 March 2022; received in revised form 28 June 2022; accepted 30 June 2022

KEY WORDS

AAV vectors;
Capsid engineering;
Vaccine;
Antigen structure design;
SARS-CoV-2

Abstract Due to the insufficient long-term protection and significant efficacy reduction to new variants of current COVID-19 vaccines, the epidemic prevention and control are still challenging. Here, we employ a capsid and antigen structure engineering (CASE) strategy to manufacture an adeno-associated viral serotype 6-based vaccine (S663V-RBD), which expresses trimeric receptor binding domain (RBD) of spike protein fused with a biological adjuvant RS09. Impressively, the engineered S663V-RBD could rapidly induce a satisfactory RBD-specific IgG titer within 2 weeks and maintain the titer for more than 4 months. Compared to the licensed BBIBP-CorV (Sinopharm, China), a single-dose S663V-RBD induced more endurable and robust immune responses in mice and elicited superior neutralizing antibodies against three typical SARS-CoV-2 pseudoviruses including wild type, C.37 (Lambda) and B.1.617.2 (Delta). More interestingly, the intramuscular injection of S663V-RBD could overcome pre-existing immunity against the capsid. Given its effectiveness, the CASE-based S663V-RBD may provide a new solution for the current and next pandemic.

*Corresponding author. Tel./fax: 86 28 85502307.
E-mail address: sunxun@scu.edu.cn (Xun Sun).
[†]These authors made equal contributions to this work.

Peer review under responsibility of Chinese Pharmaceutical Association and Institute of Materia Medica, Chinese Academy of Medical Sciences

https://doi.org/10.1016/j.apsb.2022.07.004

Please cite this article as: Wu Fuhua et al., Single-shot AAV-vectored vaccine against SARS-CoV-2 with fast and long-lasting immunity, Acta Pharmaceutica Sinica B, https://doi.org/10.1016/j.apsb.2022.07.004

1. Introduction

As of March 2022, more than 450 million cases of severe acute respiratory syndrome coronavirus 2 (SARS-CoV-2) and 6 million deaths have been confirmed (WHO Coronavirus (COVID-19) Dashboard)[1]. Although various vaccines based different strategies have been approved for prevention and control of the coronavirus disease 2019 (COVID-19) pandemic, the virus-caused infection and deaths are still rapidly growing. This situation could be partly attributed to the limitations of the current COVID-19 vaccines, such as the lack of rapid and long-term protection and deteriorated effectiveness to highly infectious variants[2−5]. Additionally, the strict requirements for multiple injections and the cold chain storage, as well as potential side effects have decreased the vaccination coverage rates. For example, the mRNA-1273 (Moderna, USA) needs to be stored at −80 °C[6]. The majority of marketed vaccines require 2 or 3 doses of vaccinations and the immune responses were generally weak after the first dose[7−11]. Additionally, ChAdOx1 nCoV-19 (AstraZeneca, UK) has been reported to cause thrombocytopenia and thromboembolic events. Hence, the development of a safe and fast response vaccine with a longer protection and better stability is still urgently needed.

Owing to its universally acknowledged safety and long-lasting transgene expression properties, adeno-associated virus (AAV), a single-stranded DNA parvovirus, has been emerged as the most promising viral vector in the field of gene therapy. Based above properties, AAV also holds a great potential to be developed as a safe and long-acting vaccine. But because of the poor capacity to induce cellular immune response even the immune tolerance of the host to the transgene products, the development of AAV-based vaccine used to be overlooked. Nowadays with immunological advances of AAV, researchers gradually revealed that the intrinsic impact factors of AAV vaccines development, including subcellular localization of encoded products, serotypes, and the capsid-specific immunity, could significantly shape the type, strength and side effects of immune outcomes. For example, the dose of antigen was related to modulating the bias in Th1/Th2 immune response[12], and the localization change of encoded antigen from cytoplasmic to membrane-bound could break the tolerance of host. AAV vaccines that have excellent transduction efficiency of APCs, especially dendritic cells (DCs), were able to improve antigen-specific T cell immune response[13]. Besides, the capsid-specific immunity which included neutralizing antibodies (NAbs) and cytotoxic T lymphocyte could block the viral transduction or even eliminate the transduced cells[14,15]. On the other hand, the delivery route could greatly affect the strength of host immune responses and determine the side effects caused by the capsid-specific immunity. Interestingly, the presence of pre-existing NAbs appeared to have no effect on transgene expression by intramuscular re-administration of the original vector[16]. However, intramuscular administration of AAV vectors could induce a vibrant antigen-specific humoral response but minimal cytotoxic T lymphocytes[17]. As IM injection is the most common administration route for vaccination, exploring appropriate strategies that can improve anti-transgene cellular immune responses and overcome the capsid-specific immune response is crucial for an AAV-based vaccine development.

Here, we hypothesize that a combined strategy of viral capsid and antigen structure engineering (CASE) may provide a target product. On the one hand, we selected AAV6 as the vaccine vector based on its excellent infection efficiency of DCs and the ability to generate cytotoxic effector and memory T cells against the transgene[16,18,19]. In addition, previous studies demonstrated that a capsid-optimized AAV6 vectors (AAV6-S663V) could further improve the transduction efficiency in DCs and the activation of CD8+ T cells[13,18]. Therefore, we replaced correspondingly the surface-exposed hydroxyl containing serine to valine at the 663 residue. At the same time, we propose to improve the antigen protein expression efficacy in the injection site and abate the immunogenicity of capsid *in vivo* by inhibiting the ubiquitination-mediated degradation of surface-exposed hydroxyl containing serine as reported[20−22]. On the other hand, receptor binding domain (RBD) of the spike protein is an ideal target for SARS-CoV-2 vaccine development as RBD is responsive for the infection *via* binding to the receptor angiotensin-converting enzyme 2 (ACE2) of host cells[23]. Meanwhile, RBD could elicit high-quality NAbs and avoid the potential risk of antibody-dependent enhancement (ADE) mediated by binding antibodies without the neutralizing activity[24,25]. In the current study, we further optimized RBD to improve its immunogenicity by a T4 fibritin-derived domain to mimic the natural trimeric viral conformation and co-expression an biological adjuvant RS09 at C-terminus[26,27], and tagged the tissue plasminogen activator (tPA) signal peptide at its N-terminus for protein to be secreted across the cell membrane.

At last, published clinical and non-human primates COVID-19 data demonstrated the levels of RBD-specific humoral and cellular responses were highly correlated with the protective immunity[11,28−30]. We introduced a licensed inactivated vaccine BBIBP-CorV (Sinopharm, China) with a half-adult dose program as the positive control, and then comprehensively compared the levels of RBD-specific humoral and cellular responses of BBIBP-CorV with AAV-based vaccines. Furthermore, we evaluated the impact of capsid immunity, the preliminary safety profile and the storage stability of AAV-based vaccines. Our results showed that the novel single-injection AAV-based vaccines hold a great potential for clinical application.

2. Materials and methods

2.1. Materials

Benzonase was purchased from Novoprotein (Suzhou, China, #M056-01). Deoxycholic acid (#30970) and beta-mercaptoethanol (#M3148) were purchased from Sigma (St. Louis, MO, USA). Poloxamer 188 was purchased from BSAF (Germany, Art 50259527, #67056). Recombinant SARS-CoV-2 spike RBD recombinant protein was purchased from Sino biological (Beijing, China, #40592-V08H). The information of all flow cytometry antibodies is listed in supplementary materials (Supporting Information Table S1). The Milli-Q water (≥18 megohm.cm) water were used in all experiments for preparing all corresponding solutions. Specific pathogen-free (SPF) 6−8-week-old female BALB/c mice were purchased from Dashuo Laboratory Animal Technology Co., Ltd. They were housed under SPF conditions, with 12-h light cycles and free access to regular chow diet and water, in the laboratory animal facilities at West China School of Pharmacy, Sichuan University. Animal studies were approved by the Committee on the Ethics of Animal Experiments of Sichuan University and conducted in compliance with the recommendations in the Guide for the Care and Use of Laboratory Animals of Sichuan University Ethics Committee.

Please cite this article as: Wu Fuhua et al., Single-shot AAV-vectored vaccine against SARS-CoV-2 with fast and long-lasting immunity, Acta Pharmaceutica Sinica B, https://doi.org/10.1016/j.apsb.2022.07.004

2.2. Cells and pseudoviruses

Human embryonic kidney cells 293T (HEK293T cells) (ATCC) and ACE2-293T cells (Suzhou, GENEWIZ, China) were maintained in Dulbecco's modified Eagle's medium (DMEM, Gibco, USA). BMDCs were isolated from C57BL/6 and cultured in RPMI1640 (Gibco, USA). All mediums were supplemented with 10% fetal bovine serum (FBS, ExCell Bio, China, #FSP500) and 1% penicillin and streptomycin. WT, C.37(Lambda) and B.1.617.2(Delta) SARS-CoV-2 pseudovirus (GENEWIZ) bearing the full-length spike protein of SARS-CoV-2 produced in an Env-defective, luciferase-expressing HIV-1 backbone.

2.3. Construction and preparation of AAV6-based vaccine plasmids

The codon-optimized RBD gene of SARS-CoV-2 spike (Gene ID: 43740568) based on the Wuhan-Hu-1 strain (NC_045512.2) was cloned into a pAAV-CAG-GFP. For this construct, a tPA signal peptide with KOZAK sequence was added to the protein N terminus to increase protein expression and secretion. Then we fused the original RBD sequence (330−583aa) with the bacteriophage T4 fibritin trimerization domain. Furthermore, RS09 was integrated into the C-terminus of antigen.

For the capsid plasmid construct design, a two-step mutagenesis protocol was performed with plasmids pAAV6 (Addgene, #110770) as guidelines described using Phusion site-directed mutagenesis kit (Thermo scientific, USA, #F541). Briefly, in step one, target plasmid was amplified by two 5' end phosphorylated primers for 24 cycles. In step two, the PCR product was digested by DpnI enzyme at 37 °C for 15 min, followed by T4 ligation to circularize plasmid in a 5-min reaction. Primers were designed to introduce change from serine (TCG) to valine (GTG) at the 663 residue. The helper plasmid of pAdDeltaF6 (#112867, encoding adenovirus E4, E2A and VA) and the reporter gene plasmid pAAV-CAG-Fluc (#83281, encoding firefly Luciferase) were purchased from Addgene. All the mentioned plasmids replaced antibiotic resistance from ampicillin to kanamycin.

2.4. Production and purification of recombinant AAV vectors

Recombinant AAV vectors were generated as described previously by triple transfection of HEK293 cells using Polyethylenimine (linear, MW 40,000; Polysciences, USA, #24765-1). The transfected cells were harvested 72 h after transfection, and cells were pelleted at 3000×*g* for 5 min and resuspended in TNE buffer (100 mmol/L Tris−HCl, pH 8.0, 150 mmol/L NaCl, 20 mmol/L EDTA) and subjected to 3 freeze−thaw cycles. The crude lysates of containing AAV were treated with Benzonase and 10% deoxycholic acid at 37 °C for 1 h to degrade unpackaged AAV DNA and centrifuged at 10,000×*g* for 30 min. At the same time, AAV released into the culture medium were recovered by addition of PEG/NaCl solution [10% polyethylene glycol 8000 (*w*/*v*), 0.5 mol/L NaCl] and subsequent precipitation at 4 °C for 16 h.

Prior to AAV purification, the resuspended buffer of containing AAV was purified by iodixanol (Sigma, USA, #D1556) gradient centrifugation followed by affinity chromatography (Thermo, USA, POROS™ CaptureSelect™ AAVX Affinity Resin, #A36745). For affinity chromatography, the solution after ultra-high-speed centrifugation was diluted 1:1 in 1 × TNK buffer (5 mmol/L KCl, 135 mmol/L NaCl, 10 mmol/L Na_2HPO_4, 2 mmol/L KH_2PO_4, 1 mmol/L $MgCl_2$). The 5 mL of resin that contains beads with the covalently bound nanobodies was added to empty gravity chromatography columns. Each affinity column was equilibrated with 15 column volumes of 1 × TNK buffer prior to loading of the solution. Following sample loading, the columns were washed with 25 mL of 1 × TNK buffer and subsequently eluted with 0.1 mol/L glycine-HCl (pH 2.6). The eluate was immediately neutralized with 1 mol/L Tris−HCl (pH 10). For virus purity determination, it was confirmed by SDS-PAGE (protein silver stain) and negative stain TEM (Transmission Electron Microscope). The AAVs were dialyzed in stock buffer (20 mmol/L Tris-Cl pH 8.0, 180 mmol/L NaCl, 1 mmol/L $MgCl_2$, 0.003% Poloxamer 188) by using Slide-A-Lyzer™ Dialysis Cassettes (Thermo, 20K MWCO, 12 mL, #66012). Titers of the vectors were determined by TaqMan qPCR with the following primer pairs. Primer pair for RBD: forward 5'-TTCAACGCCACAAGATTCGC-3', reverse 5'- TTGGTGAAGCACAGGTCGTT-3' and TaqMan probe FAM-AAGAATCAGCAACTGCGTGGCCG-BHQ1. Primer pair for GFP: forward 5'-CACATGAAGCAGCACGACTT-3', reverse 5'- TCGTCCTTGAAGAAGATGGT-3' and TaqMan probe FAM-AGTCCGCCATGCCCGAAGGCT-BHQ1. Primer pair for Luc: forward 5'-CGCACATATCGAGGTGGACA-3', reverse 5'- GCAAGCTA-TTCTCGCTGCAC-3' and TaqMan probe FAM-TTCGAGATGAGCGTTCGGCTGGC-BHQ1.

2.5. Western blot

The expression of antigen was evaluated by Western blot[31], HEK293T cells were transduced with 40,000 multiplicity of infection (MOI) of rAAV6 WT-RBD or rAAV6 S663V-RBD. At 48 h after infection, the culture supernatant and lysates of HEK293T were separately mixed with sample loading buffer with or without beta-mercaptoethanol (β-ME) and heated for 10 min at 95 °C. The proteins were separated by 10% SDS-PAGE gels and then transferred to polyvinylidene fluoride (Millipore, USA, 0.2 μmol/L PVDF, #ISEQ00010) membrane. After blocking for 1 h at room temperature with 5% skim milk in TBST, membranes were incubated with anti-SARS-CoV-2 spike mouse monoclonal antibody (1:2000, Sino Biological, China, # 40591-MM42) overnight at 4 °C, and then washing three times with TBST. Membranes were incubated with Horseradish peroxidase (HRP)-conjugated goat anti-mouse IgG (1:20,000, thermo, USA, #31431) at RT for 2 h. After repeating washing procedure, the signals were visualized using ECL substrate reagents (Millipore, USA, WBKLS0100) and acquired with a Clinx ChemiDox imaging system (Bio-Rad, USA).

2.6. Assays of singleton modification vectors transduction efficiency to bone marrow−derived DCs (BMDCs)

BMDCs were obtained as described previously[32]. Briefly, 8-week-old male C57BL/6 mice were sacrificed to isolate bone marrow cells of femur and tibia. Then, bone marrow cells were cultured for 7 days in RPMI 1640 medium (Gibco, USA) supplemented with 10% heat-inactivated FBS, 20 ng/mL GM-CSF (R&D Systems, USA) and 50 μmol/L β-mercaptoethanol. The purity of BMDCs was characterized by measuring the percentage of typical phenotype ($CD11c^+$) cells. The cells of which positive percentage was higher than 85% was applied for the following transduction assays. Qualified BMDCs were infected by WT-GFP or S663V-GFP with MOI 20,000. Transduction efficiency was measured as

Please cite this article as: Wu Fuhua et al., Single-shot AAV-vectored vaccine against SARS-CoV-2 with fast and long-lasting immunity, Acta Pharmaceutica Sinica B, https://doi.org/10.1016/j.apsb.2022.07.004

integrated green fluorescence density per cell (mean ± SEM) by Image J software.

2.7. Inoculation of mice

For optimizations on the serotype of vector, BALB/c mice were injected intramuscularly (i.m.) with 8×10^9 vector genomes (VG) of rAAV5 WT-Luc, rAAV6 WT-Luc or rAAV8 WT-Luc ($n = 5$ per group) and its luminous signal was gathered by the IVIS Lumina III system (PerkinElmer, USA). Another batch of BALB/c mice were vaccinated intramuscularly with 1×10^{11} VG of rAAV6 WT-RBD or rAAV6 S663V-RBD ($n = 12$ per group) and same dose rAAV6 WT-GFP or rAAV6 S663V-GFP vectors as negative controls ($n = 9$ per group). Mice were injected intraperitoneally (i.p.) with two-dose BBIBP-CorV using 2 μg/dose on Days 0 and 21 as positive control ($n = 6$ per group). After 14 days of initial inoculation, three rAAV6 WT-GFP and three rAAV6 S663V-GFP were sacrificed to evaluate the infectivity of vector and its immune stimulation. Serum was collected for RBD-specific ELISA and SARS-CoV-2 PNAb titration at different time points. After 10 weeks of initial vaccination, each group mice were euthanized for detecting the splenic T-cell response, drain lymph nodes germinal center reaction, and safety profile, and the remaining rAAV6 WT-RBD or rAAV6 S663V-RBD ($n = 6$ per group) continued to be fed for the investigation of long-term immune response.

For evaluating the transgene expression kinetics of S663V mutants, BALB/c mice ($n = 4$ per group) were injected intramuscularly with 1×10^{10} VG of rAAV6 WT-Luc or rAAV6 S663V-Luc.

For investigation of the impact of pre-existing antibodies, BALB/c mice ($n = 4$ per group) were immunized intramuscularly with 5×10^{10} VG of rAAV6 WT-GFP or rAAV6 S663V-GFP, and mice were vaccinated at same site with 1×10^{11} VG of WT-RBD or S663V-RBD 14 days after first vaccination. Serum was collected for capsid-specific and RBD-specific ELISA at intended time points.

2.8. Enzyme-linked immunosorbent assays (ELISAs)

SARS-CoV-2 RBD-binding antibody titers was detected by ELISAs[33], 96-well high binding plates (Corning, USA, #9018) were coated at 4 °C with 80 ng/mL of SARS-CoV-2 spike RBD recombinant protein (Sino biological, China, #40592-V08H) overnight. Plates were washed twice with PBS containing 0.05% Tween 20 (PBS-T) and blocked with PBS pH 7.4 in 1% BSA at 37 °C for 1.5 h and washed again. After Mouse serum samples were 3-fold serially diluted from 1:30 in PBS-T containing 1% BSA. After 2 h of incubation at 37 °C, plates were washed with PBS-T five times and 100 μL HRP-conjugated goat anti-mouse IgG, IgG1 and IgG2a (1:10,000, Abcam, UK, #ab98731, #ab98693 and #ab98698) added to each well and incubated at 37 °C for 1.5 h. The plates were washed and 100 μL TMB peroxidase substrate solution (InnoReagents, China, # EL0001) was added. The reaction was stopped by the addition of 50 μL of 2 mol/L H_2SO4 and then measured optical density (OD) at 450 nm (TECAN, Switzerland). The endpoint titer was defined as the highest reciprocal serum dilution that yielded an absorbance ≥2.1-fold over the average values of negative control samples.

2.9. SARS-CoV-2 pseudovirus neutralization assay

The 50% tissue culture infectious dose (TCID50) of a single thawed aliquot of each batch of pseudovirus was determined in ACE2-293T cells. For TCID50 measurements, serial threefold dilutions of pseudoviruses were made in octuplicate wells in 96-well culture plates in a total volume of 50 μL of complete medium for a total of 8 dilutions. An equal volume of freshly trypsinized cells (15,000 cells) were added to each well, and the plates were incubated for 48 h at 37 °C in 5% CO2 air environment. Then, 100 μL of Bright Glo luciferase substrate (Promega, USA, #E2620) was added to each well. Two min after incubation at room temperature, 150 μL of lysates was transferred to white solid 96-well plates (NUNC, USA, #463201) for the detection of luminescence using a microplate luminometer (Thermo, USA). The positive well was determined as 10-fold relative luminescence unit (RLU) values higher than the cell background. The 50% tissue culture infectious dose (TCID50) was calculated using the Reed−Muench method.

To evaluate the pseudovirus neutralization activity of mouse serum which was heated at 56 °C for 30 min, sera were 4-fold serially diluted from 1:20 and incubated with an equal volume of 100 $TCID_{50}$ pseudovirus at 37 °C for 1 h. The medium was mixed without pseudovirus as a negative control. Then the mixture was added to each well with freshly trypsin-treated cells. After incubation for 48 h, the luciferase activity was measured as described in the section for pseudovirus TCID50 titration. The 50% inhibitory dilution (IC50) was calculated with non-linear regression, *i.e.*, log (inhibitor) response (four parameters), using GraphPad Prism 9.0.

2.10. IFNγ Elispot and cytokine secretion in splenocytes

RBD-specific T lymphocyte immune responses were detected by a Dakewe IFNγ ELISPOT Kit (Dakewe, China) as described previously[34]. Briefly, mice spleens were grinded through a 70 μmol/L cell strainers in 5 mL 1 × Mouse Lymphocyte Separation Medium (Dakewe). Then the tissue grinding fluid was centrifuged at 500×*g* for 5 min and the pellets were lysed by ACK lysis buffer for 8 min. The isolated splenocytes were then counted for this assay and the following experiments. 1×10^6 of spleen lymphocytes were seeded into each well of a pre-coated 96-well ELISpot plate and only stimulated with RBD major histocompatibility complex (MHC) class I peptides (GL Biochem, China) for 24 h at 37 °C with 5% CO2. Then the biotinylated antibody and streptavidin-HRP was added into the plate one after another. The AEC substrate buffer were used to develop spots, and the counts were quantified by an AID ELISPOT reader.

8×10^6 freshly isolated splenocytes were stimulated with RBD protein and MHCI peptides as described previously. After incubation for 72 h at 37 °C, the culture supernatants were collected and cytokines concentrations were measured by Mouse IL-2/IL-4/IL-6/IL-12/IL-17/TNFα/IFNγ Uncoated ELISA Kit (Invitrogen, USA) after two-fold dilution, respectively.

2.11. Germinal center (GC) responses and memory T cell phenotyping

Germinal center responses were assessed as described previously[35]. Briefly, popliteal and inguinal lymph nodes (LNs) were homogenized to obtain single cell suspensions with a syringe plunger and filtered with a 70-μm cell strainer. After that, cells were incubated with a cocktail of fluorescently labeled anti-mouse monoclonal antibodies (mAbs) including CD19-PE, GL7- Alexa Fluor 488 and B220-Alexa Fluor 647 in fluorescence-activated cell sorter (FACS) buffer (PBS with 2% FBS) for 45 min.

For memory T cell phenotyping, isolated splenocytes were stimulated as described in cytokine secretion detection and stained

Please cite this article as: Wu Fuhua et al., Single-shot AAV-vectored vaccine against SARS-CoV-2 with fast and long-lasting immunity, Acta Pharmaceutica Sinica B, https://doi.org/10.1016/j.apsb.2022.07.004

with a mixture of fluorescently labeled anti-mouse mAbs containing CD4-APC eFluor780, CD8a-FITC, CD44-APC and CD62L-PE/Cy5 in FACS buffer for 30 min.

2.12. Intracellular cytokine staining of splenocytes

The RBD-specific stimulation of isolated spleen lymphocytes was performed as described in cytokine secretion detection and positive controls were stimulated eBioscience Cell stimulation cocktail (Invitrogen, USA, #00−4975). After 1 h incubation, 1000 × Brefedin A (Thermo, USA, #00-4506-51) was added to the culture to block cytokine secretion and the samples were incubated for further 4 h. After stimulation, the cells were collected and stained with a cocktail of surface markers antibodies including CD4-APC eFluor780 and CD8a-FITC for 30 min at 4 °C. Following twice washes, the cells were fixed with IC Fixation Buffer (Invitrogen, USA). For 20 min at RT and permeabilized with Cytoperm (Invitrogen, USA). Then the cells were stained with IFNγ-APC, TNF eFluor450, IL-2 Per CP/Cy5.5, IL-4-PE in Cytoperm for 30 min at RT.

All stains were stopped with twice pre-cold PBS washes and the cells were resuspended in appropriate volume PBS, and data were acquired on BD FACSCelesta (BD Biosciences, USA).

2.13. Safety assays

Lungs, hearts, livers, kidneys and injected gastrocnemius muscle from mice were collected and fixed in 4% paraformaldehyde for 24−48 h. Thereafter, tissues were embedded into optimum cutting compound (paraffin) and trimmed to twenty serial 10-μm-thick sections. The respective tissue slides were stained with hematoxylin and eosin (H&E) and photographed for histopathological analysis. To evaluate systemic safety, fresh blood was gathered to perform routine blood tests according to instruction manual.

2.14. Stability assays

The stability of the vectors was assessed by detecting the transduction activity *in vivo* and *in vitro*. The purified vectors were removed from −80 °C refrigerator and stored at 4 °C for 0, 10, 20 or 35 days, respectively. For *in vitro* detection, HEK293T cells were infected with MOI 20,000 of rAAV6 WT-GFP or rAAV6 S663V-GFP. After 48 h incubation, the transduced cells were imaged by confocal microscope (Zeiss, Germany) and trypsinized to perform FACS analysis. The results were normalized to the percentage of cells infected with virus vectors stored at −80 °C. For *in vivo* detection, mice were intramuscularly injected with 1×10^9 VG of WT-Luc or S663V-Luc. After 7 days, the luminous signal was gathered.

2.15. FACS gating strategy

At least 800,000 events were collected for each *in vivo* sample, and at least 40,000 events for each *in vitro* sample. All data were analyzed by FlowJo v10 software. Forward scatter height (FSC−H)-*versus*-forward scatter area (FSC-A) and side scatter area (SSC-A)-*versus*-FSC-A plots were used to exclude doublets and focus on live single lymphocytes.

GC B cell: B cells were gated from $B220^+$ live single cells, GC B cells were defined as $GL7^+$ and $CD19^+$.

Memory T cell phenotype: $CD44^+$ and $CD62L^+$ cells were gated from $CD4^+$ or $CD8^+$ live single T cells. Central memory T cells (TCM) were defined as $CD44^+/CD62L^+$.

ICS: Cytokine-positive cells were gated from $CD8^+$ or $CD4^+$ live single cells.

In vitro infection efficiency: GFP^+ cells were gated from live single HEK293T cells.

2.16. Statistical analysis

The analyses were performed with GraphPad Prism v.9.0. Two-tailed Student's *t*-test was performed to compare differences between two unpaired experimental groups. One way-ANOVA or two way-ANOVA with Dunn's or Tukey's multiple comparisons tests were conducted to compare differences among multiple unpaired experimental groups, One way-ANOVA with Šídák's multiple comparisons test or Bartlett's test were also applied to compare differences among multiple groups. Statistical significance was set at the critical values of $^*P < 0.05$, $^{**}P < 0.01$, $^{***}P < 0.001$, $^{****}P < 0.0001$.

3. Results

3.1. Optimizations on the serotype of vector

Published studies demonstrated that AAV5 and AAV8 could generate robust and long-term protective immunity against antigens[36,37]. Thus, we compared the intensity of luminous signal at injected tissue and liver to evaluate the transgene production and hepatotoxicity. Overall, AAV6 shows the highest muscle transduction efficiency and a relatively low liver tropism with 8×10^9 VG (Fig. 1A). The average radiance of injected muscle of AAV6 is more than 20 times that of AAV8 and 150 times that of AAV5 on Day 4 (Fig. 1B) and more than 30 times that of AAV8 and 80 times that of AAV5 on Day 7 (Fig. 1C). Moreover, there was no significant difference of liver among all groups on Day 4, but the luminescence of liver of AAV8 is visible on single image (data not shown) and higher than 8 times that of AAV6 on Day 7. Our results show that compared with AAV8 and AAV5, AAV6 can express the transgene more efficiently and rapidly at the injection site, which is conducive to establish a rapid antigen-specific immune response. In addition, AAV6 has lower hepatotropism than AAV8, indicating a lower hepatotoxicity of AAV6. Meanwhile, AAV8-based vaccine could not induce vibrant cellular immune response and the infectivity of AAV5 on mature and immature DCs was significantly lower than that of AAV6[36,38,39]. To sum up, we select AAV6 for follow-up study.

3.2. Designation and characterization of AAV-based vaccines

We first engineered the antigen fused with adjuvant structure and the capsid of the AAV. To design an ideal antigen-expression cassette, tPA signal peptide, T4 fibritin-derived trimeric motif and a specific element RS09 with adjuvant function were fused to the condon-optimized RBD sequence (Fig. 2A). Meanwhile, we introduced a capsid-exposed site mutation to 663 residues (mutating serine to valine, S663V) that are located on the 5-fold symmetry axis of AAV. The three-dimensional structure of AAV6 (PDB: 3OAH) was shown (Fig. 2B). After the purification by iodixanol density gradient centrifugation and the AAVX affinity chromatography, the transmission electron microscopy (TEM) and the SDS-PAGE silver stain were used to evaluate the quality of wild type AAV6 (WT-RBD) and AAV6-S663V (S663V-RBD). The results indicated that the generated WT-RBD and S663V-RBD had excellent purity and a low empty shell rate,

Please cite this article as: Wu Fuhua et al., Single-shot AAV-vectored vaccine against SARS-CoV-2 with fast and long-lasting immunity, Acta Pharmaceutica Sinica B, https://doi.org/10.1016/j.apsb.2022.07.004

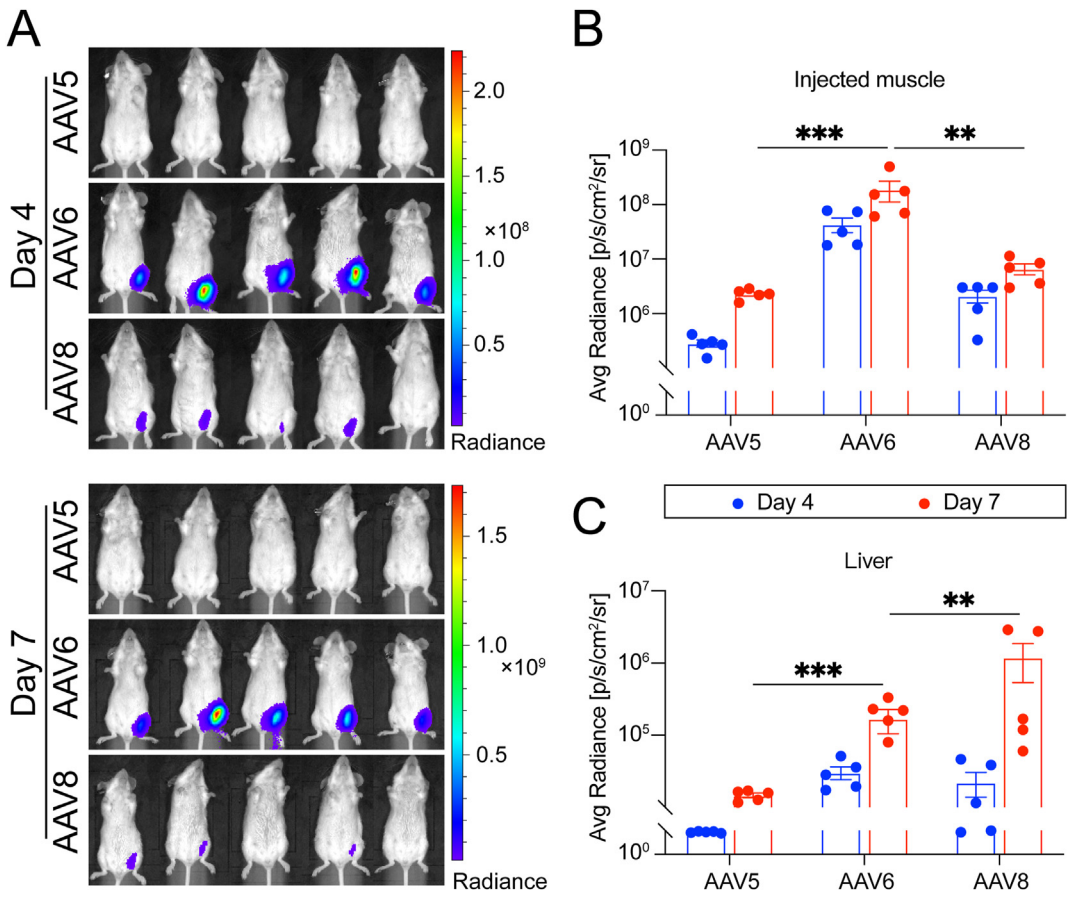

Figure 1 Optimizations on the Serotype of Vector. (A) The luminescence images of injected animals. BALB/c female mice (6−8 weeks old) were injected intramuscularly (i.m.) with 8×10^9 VG of AAV5-Luc, AAV6-Luc or AAV8-Luc. The intensity of luminescence at injected muscle (B) and liver (C) at intended time point, $n = 5$. Data are presented as mean ± SEM. Statistical significance was determined by one-way ANOVA with Bartlett's test. $^*P < 0.05$, $^{**}P < 0.01$, $^{***}P < 0.001$.

which was beneficial for us to conduct follow-up experiments (Fig. 2C−D). We next confirmed the secretory expression of trimer RBD of the designed AAV6 vaccine with Western Blot. The molecular-weight of the bands was closed to 140 kDa (no pretreatment) and 45 kDa (pretreated by β-ME), representing trimer and monomer, respectively (Fig. 2E). In this study, to evaluate the superiority of capsid modification and predict the enduring effectiveness of AAV-based vaccines, we investigated the expression kinetics of intramuscular luciferase (Luc) by quantifying the chemiluminescence signal. The results demonstrated that S663V mutants could improve transduction efficiency about 2-fold when compared with WT at the same dose and the transgene could constantly express for more than 270 days (Fig. 2F). Meanwhile, we investigated the transduction efficacy of S663V mutants to BMDCs and visualized its immune organs stimulation response and infectivity *in vivo via* injected intramuscularly with 1×10^{11} VG WT-GFP or S663V-GFP. Our results indicate S663V could significantly improve transduction efficiency to BMDCs when compared to WT (Supporting Information Fig. S1). Within two weeks, transgene could be expressed at almost completely injected gastrocnemius and energetically stimulate the draining LNs enlargement (Supporting Information Figs. S2A and S2B).

All these above results indicate that we have successfully fabricated WT-RBD and S663V-RBD with a high purity that could more efficiently express secretory trimeric RBD with a strong infective activity.

3.3. Single dose of S663V-RBD elicited a rapid robust and balanced immune response over time

To investigate the capacity of S663V-RBD to induce humoral immune responses, we first screened the dose of our vaccine for immunization. The dose of 1×10^{11} VG was able to induce the highest level of RBD-specific immunoglobulin G (IgG) and subtype antibodies (IgG ∼4.8, IgG1 ∼4.6 and IgG2a ∼4.6) within 2 weeks (Supporting Information Fig. S3). The humoral immune response of the licensed inactivated vaccine BBIBP-CorV (Sinopharm, China) would peak at 7 days after second dose boosting (at about week 4)[40]. Therefore, we measured RBD-specific antibodies by ELISAs at Week 4−10 after the initial immunization (Fig. 3A). WT-RBD and BBIBP-CorV were used as control groups. Overall, the endpoint titer of RBD-specific IgG, IgG1 and IgG2a among BBIBP-CorV, WT-RBD and S663V-RBD showed two distinct trends. The titer of BBIBP-CorV group after two doses quickly reached ∼5.6 at Week 4, but gradually decreased to ∼5 at Week 10. WT-RBD showed a stable antibody titer of ∼5.5 over time. By contrast, our S663V-RBD group inoculated with only a single dose showed a similar titer of ∼5.5 at Week 4 and 6 but increased to around 6 at Week 8 and 10, which was significantly higher than that of WT-RBD and BBIBP-CorV. At Week 10, S663V-RBD induced a 2−3-fold higher titers of IgG (∼5.9), IgG1 (∼6.1) and IgG2a (∼5.9) than that of WT-RBD (∼5.5, ∼5.7 and ∼5.5, respectively), 4 − 8-fold higher titers of that of BBIBP-CorV (∼5.0, ∼5.2 and

Please cite this article as: Wu Fuhua et al., Single-shot AAV-vectored vaccine against SARS-CoV-2 with fast and long-lasting immunity, Acta Pharmaceutica Sinica B, https://doi.org/10.1016/j.apsb.2022.07.004

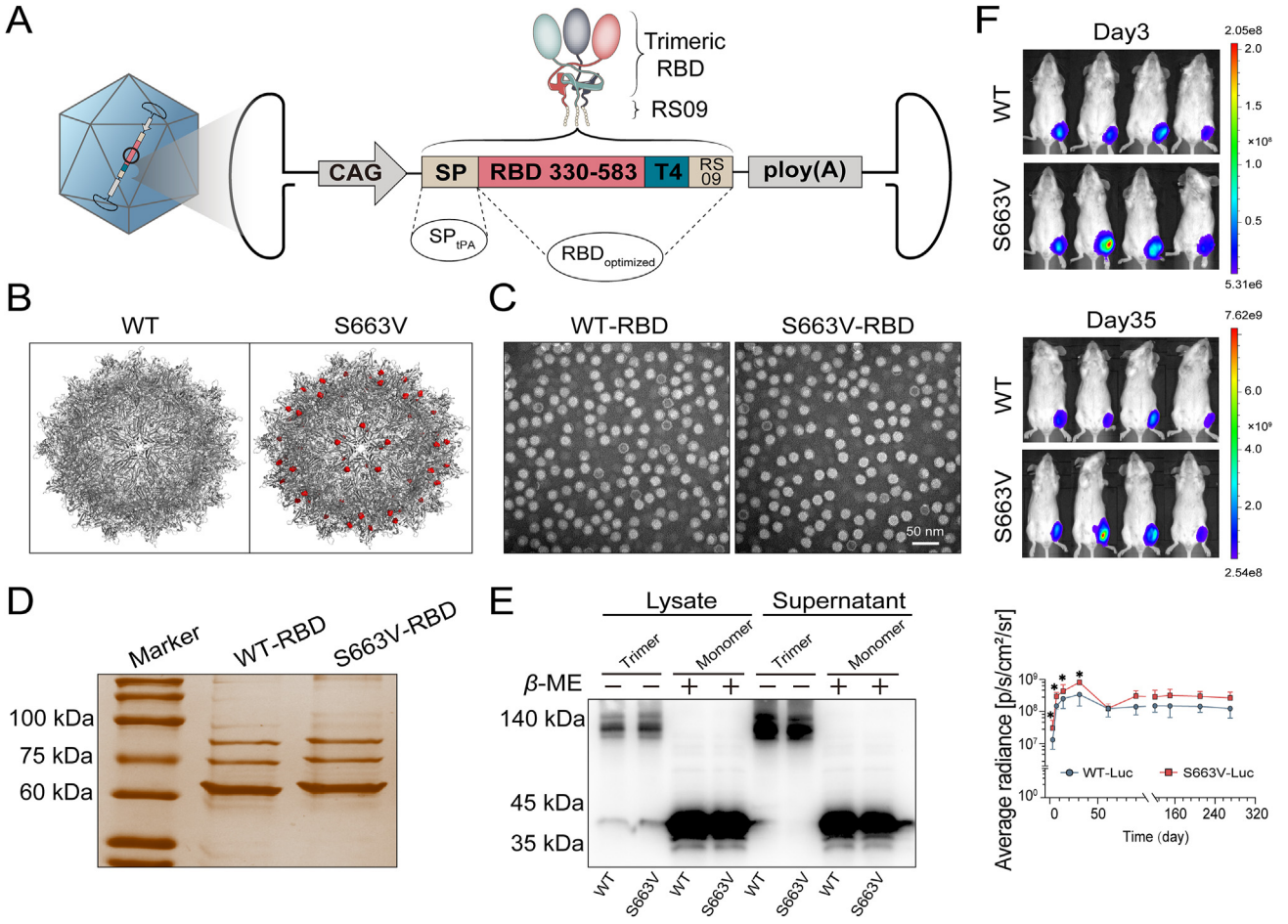

Figure 2 The design and *in vitro* characterization of AAV6-based vaccines. (A) Schematic of SARS-CoV-2 RBD antigens. (B) Three-dimensional structure of WT-RBD and S663V-RBD, red small dots indicate the mutation site at the 663 residue. (C) The morphology of WT-RBD or S663V-RBD was visualized by the transmission electron microscopy with a negative stain. (D) Virion purity was assessed by silver stain. (E) Western blot of transgene expression in cells cultures and lysates of HEK293T infected with WT-RBD or S663V-RBD with β-ME treatment or not. (F) The transgene expression kinetics. BALB/c female mice (6−8 weeks old) were injected intramuscularly (i.m.) with 1×10^{10} VG of WT-Luc or S663V-Luc, and the transgene expression were detected at intended time point, $n = 4$. Data are presented as mean ± SEM. Statistical significance was determined by unpaired Two-tailed Student's t tests. $^*P < 0.05$.

∼5.2, respectively) (Fig. 3B and C, Supporting Information Fig. S4). At Week 18, S663V-RBD maintain the titers of IgG (∼5.3), IgG1 (∼5.2) and IgG2a (∼5.5) and induced 2−3-fold higher titers than that of WT-RBD (∼5.0, ∼5.0 and ∼5.0, respectively, Supporting Information Fig. S5).

In addition, antigen-specific cellular immune responses were measured by IFNγ-specific spots produced by stimulated splenocytes from immunized animals at Week 10 after the above vaccination schedule. We found that S663V-RBD generated significantly stronger RBD-specific $CD8^+$ T cell responses when compared to WT-RBD and BBIBP-CorV (Fig. 3D).

3.4. *AAV-based vaccines provided a potent protection against multiple pseudoviruses over time*

Since previous studies indicated a strong correlation between the titer of neutralizing antibodies and the protective efficacy against SARS-Cov2 infections[29,41], we assessed the levels of pseudovirus neutralizing antibody (PNAb) titers against three typical stains (WT, Delta and Lambda) by the pseudovirus neutralization assay (Fig. 4A). For the wild type pseudovirus neutralizing assay, there was no significant difference in PNAb titer among the three groups at Week 4. However, the neutralization activity of BBIBP-CorV declined gradually from Week 4 to Week 10, showing a PNAb titer decrease from ∼4.3 to ∼3.8. This trend was consistent with that found in the antibody responses. On the contrary, the neutralization activity of AAV-based vaccine increased to ∼4.6 ($lgIC_{50}$) at around Week 6 and maintained at a high level until the end of the experiment. Importantly, S663V-RBD showed the strongest capacity to induce PNAb for neutralization of the wild type pseudovirus. At Week 10, the PNAb titer of S663V-RBD group was about 3 and 6 times of that of WT-RBD and BBIBP-CorV, respectively (Fig. 4B).

Lambda and Delta COVID-19 strains that are both highly pathogenic and highly infectious, recently spread globally and caused enormous challenges for the effective control of the epidemic[42,43]. Therefore, we selected delta and lambda for pseudovirus neutralization assays to investigate the capacity of our AAV6 vaccine to prevent variants of COVID-19. We observed significant decline of PNAb titers in all the three groups as

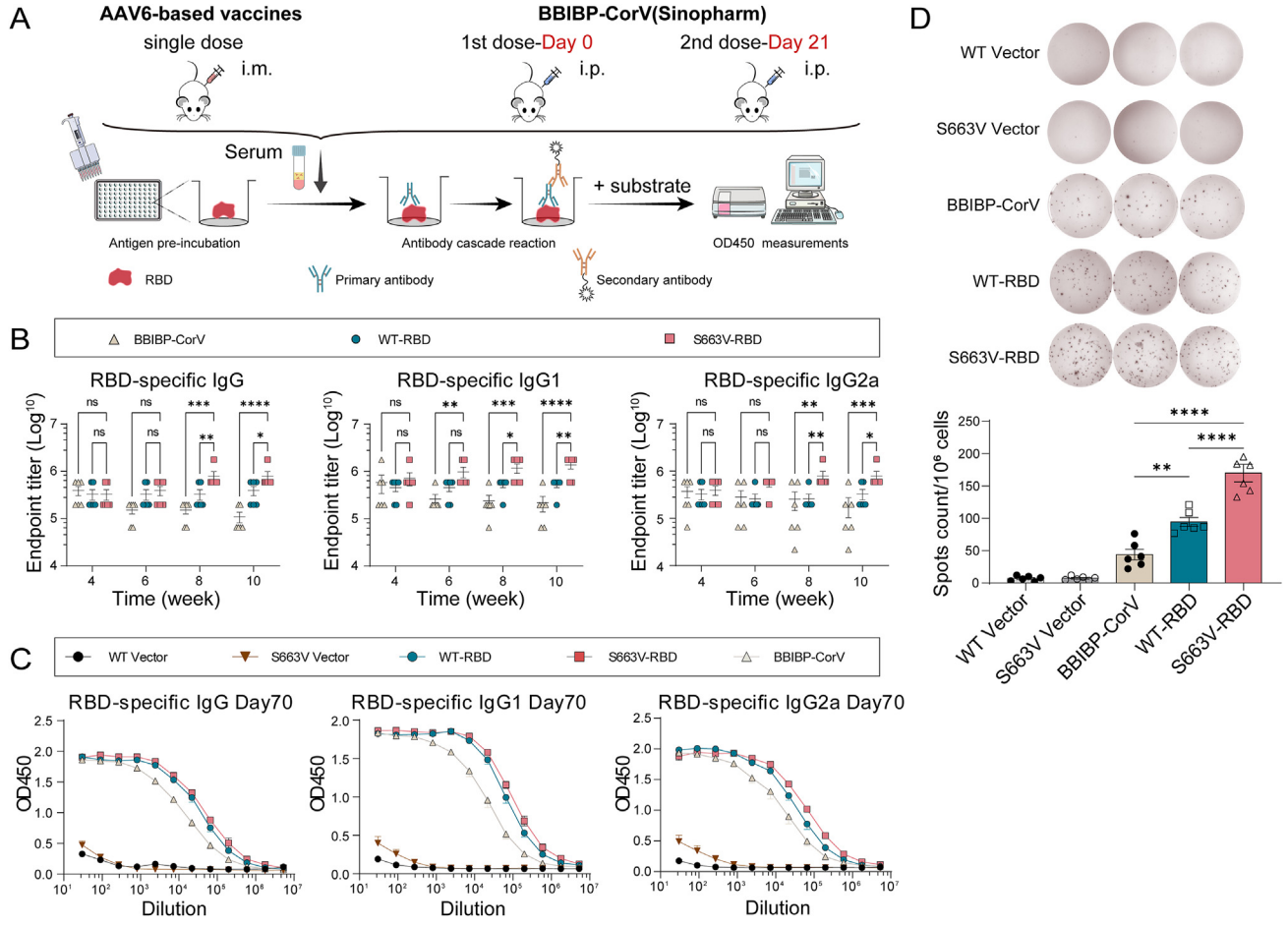

Figure 3 Single dose of AAV-based vaccines elicited a robust balance immune response over time. (A) Schematic of dose regimen and the principle of the enzyme-linked immunosorbent assays (ELISA). BALB/c female mice (6−8 weeks old) were injected intramuscularly (i.m.) with one dose (1×10^{11} VG) of WT-RBD or S663V-RBD. Negative control mice were administered the same dose of WT-GFP or S663V-GFP. Positive control mice were injected intraperitoneally (i.p.) with two-dose of BBIBP-CorV using half adult dose (2 μg/dose) on Days 0 and 21. Sera were collected at the intended time for assessing SARS-CoV-2 RBD-specific binding antibody titers, $n = 6$. (B) The endpoint titer of IgG, IgG1 and IgG2a. (C) RBD-specific binding of antibodies in serial serum dilutions from mice on Day 70. (D) IFNγ spot-forming units (SFU) of splenocytes stimulated with MHC class I RBD-immunodominant peptide. Data are presented as mean ± SEM. Statistical significance was determined by two-way ANOVA with Dunnett's multiple comparisons test (B) or one−way ANOVA with Šídák's multiple comparisons test (D). ns: not significant ($P > 0.05$), *$P < 0.05$, **$P < 0.01$, and ***$P < 0.001$.

compared to the wild type pseudovirus. For instance, the PNAb titer of BBIBP-CorV decrease from ∼4.3 to ∼2.8 (Lambda) and ∼2.9 (Delta) at Week 4, respectively. However, S663V-RBD still showed a superior PNAb against the COVID-19 variants among all the groups. At Week 10, the anti-lambda PNAb titer of S663V-RBD group was about 2- and 3-fold of that of WT-RBD group and BBIBP-CorV group, respectively. Additionally, the anti-delta PNAb titer of S663V-RBD group was about 2- and 5-fold of that of S663V-RBD and BBIBP-CorV group at week 10 (Fig. 4C and D, Supporting Information Fig. S6), respectively. Collectively, these results showed that S663V group could induce significantly higher PNAb titers as displayed in the non-linear fitting curves.

3.5. *Single dose of AAV-based vaccines generated strong GC B cell responses*

Vaccination strategies deploying one or few immunizations are an attractive option if capable of eliciting efficient immune responses. Considering the correlation of GCs for the generation of high-quality persistent neutralizing antibody responses[29,30,44], we compared the GC formation among AAV-based vaccines and BBIBP-CorV. GC B cells in draining lymph nodes (LNs) were evaluated by the flow cytometry 10 weeks after the immunization (Fig. 5A). Compared to WT-RBD and BBIBP-CorV, S663V-RBD induced the highest ratio of GC B cells ($CD19^+$ B cells) in popliteal LNs but no difference was found in inguinal LNs (Fig. 5B and C). The main reason may be that the popliteal LNs are closer to the injection site. The robust GC response also explained why S663V-RBD had the strongest neutralizing vitality among three groups.

3.6. *Single dose of AAV-based vaccines generated RBD-specific polyfunctional T-cell responses and a strong central memory T-cell response*

To assess the response to a second exposure to antigen in vaccinated mice, we compared the percentage of memory phenotypes of stimulated splenocyte based on the expression of CD44 and CD62L. The S663V-RBD produced the highest levels of $CD4^+$

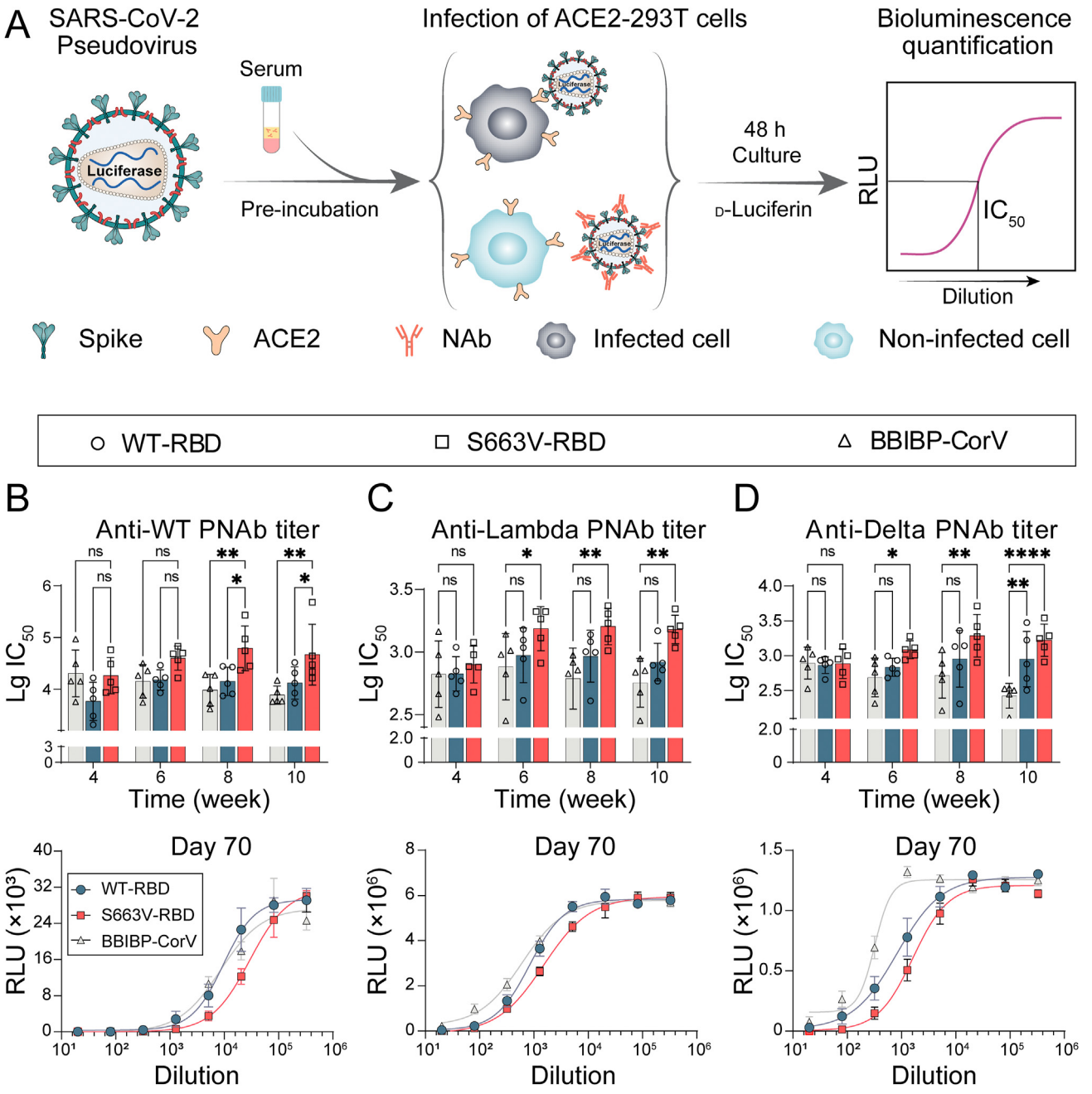

Figure 4 Single dose of AAV-based vaccines provides a potent protection of multiple pseudoviruses over time. (A) Schematic of determination principle of pseudovirus neutralizing antibody titer. (B)−(D) The 50% inhibitory dilution (IC50) against WT strain, C.37 (Lambda) and B.1.617.2 (Delta) and the corresponding relative luminescence unit (RLU) in serial serum dilutions from mice on Day 70, respectively. Data are presented as mean ± SEM. Statistical significance was determined by two−way ANOVA with Dunnett's multiple comparisons test. ns: not significant ($P > 0.05$), *$P < 0.05$, **$P < 0.01$, and ***$P < 0.001$, $n = 5$.

and $CD8^+$ central memory T cells when compared to WT-RBD and BBIBP-CorV (Fig. 5D). In addition, antigen-specific activation of T cells could play multiple functions by secreting a variety of cytokines, which could be regarded as an important indication of vaccine quality. Correspondingly, functional properties of RBD-specific T-cells responses were evaluated *via* the intracellular cytokine staining assay of splenocytes. Compared to WT-RBD, S663V-RBD induced higher levels of IFNγ, TNFα, IL-2, and IL-4 in splenic $CD8^+$ or $CD4^+$ T cells. Compared to BBIBP-CorV, S663V-RBD elicited higher levels of IFNγ and IL-2, as well as comparable levels of TNFα and IL-4 (Fig. 5E). To further investigate the production and secretion of cytokines, the concentrations of cytokines (IFNγ, TNFα, IL-4, IL-6, IL-12 and IL-17A) in the culture supernatant of stimulated splenocytes were measured after 72 h incubation. Consistent with the trend of antibody levels, the concentrations of cytokines in S663V-RBD group were significantly higher than those in the other two groups. In particular , compared to WT-RBD, S663V-RBD produced higher levels of IFNγ , IL-17A and IL-6, as well as comparable levels of TNFα and IL-4. Compared to BBIBP-CorV,

Please cite this article as: Wu Fuhua et al., Single-shot AAV-vectored vaccine against SARS-CoV-2 with fast and long-lasting immunity, Acta Pharmaceutica Sinica B, https://doi.org/10.1016/j.apsb.2022.07.004

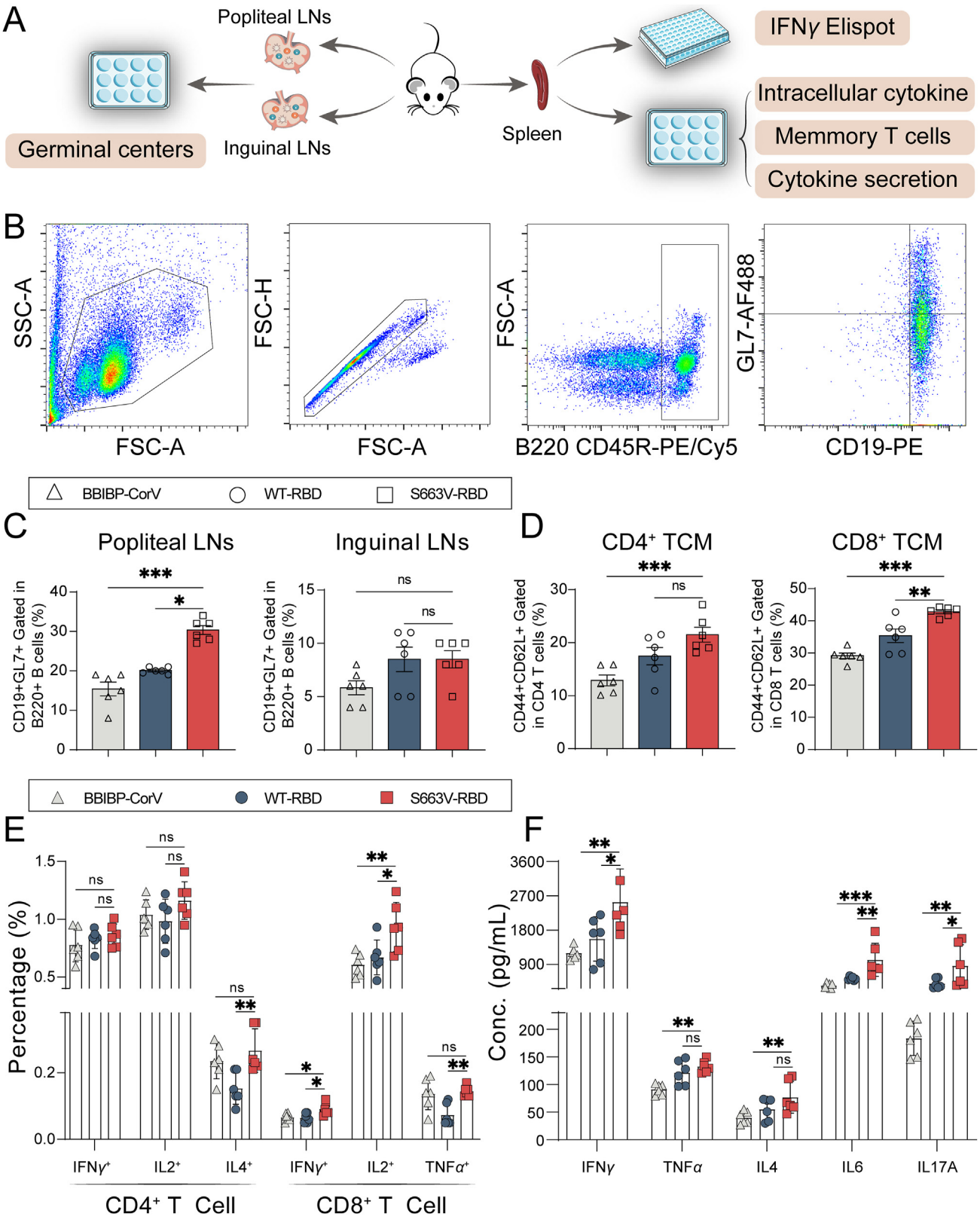

Figure 5 Single dose of AAV-based vaccines strong Germinal Center (GC) B cell responses, RBD-specific polyfunctional T-cell responses and a strong central memory T-cell response. (A) The scheme of experiments. (B) The gate strategy of GC B cell. (C) GC response in Ipsilateral draining lymph nodes of the injection site. (D) The central memory T cells responses of splenocytes. (E) RBD-specific polyfunctional $CD4^+$ and $CD8^+$ T cells responses of splenocytes. (F) The concentrations of cytokines in splenocytes culture supernatant. Data are presented as mean ± SEM. Statistical significance was determined by one−way ANOVA with Dunnett's multiple comparisons test (C− F). ns: not significant ($P > 0.05$), *$P < 0.05$, **$P < 0.01$, and ***$P < 0.001$, $n = 6$.

Please cite this article as: Wu Fuhua et al., Single-shot AAV-vectored vaccine against SARS-CoV-2 with fast and long-lasting immunity, Acta Pharmaceutica Sinica B, https://doi.org/10.1016/j.apsb.2022.07.004

S663V-RBD generated higher levels of IFNγ^+, TNFα^+, IL-4$^+$, IL-6, IL-12 and IL-17A (Fig. 5F).

3.7. *Singleton modified AAV ameliorated the impact of pre-existing immunity*

Clinically, systematic administration of AAV usually need exclude sero-positive subjects, which greatly restrict the application scope of AAV-based therapies. However, previous research demonstrated AAV vectors could re-administrate into the respiratory tract or muscles in the context of pre-existing antibodies[16,45,46]. To identify the impact of pre-existing immunity against the vector capsid, we designed a re-administration program. Mice were divided into four groups and inoculated with WT-GFP or S663V-GFP on Day 14 and with WT-RBD or S663V-RBD on Day 0, respectively (Fig. 6A). The capsid-specific NAbs on Day 0 were detected, which indicated the pre-existing immunity was successfully established and the NAbs tilter between WT and S663V showed no difference (Fig. 6B). On Day 28, in presence of pre-existing immunity, S663V-RBD vaccine *via* i.m. administration could induce robust RBD-specific antibody titers (Fig. 6C). The titers of IgG, IgG1 and IgG2a levels were ~5.6, ~5.5 and ~5.6 respectively, which were comparable to the mice vaccinated with S663V-RBD only (~5.5, ~5.8 and ~5.6, respectively in Fig. 3B). But pre-injecting with vectors significantly weakened the antigen-specific immune response (IgG ~4.9, IgG1 ~5.0 and IgG2a ~4.8, respectively) of WT-RBD on Day 28 when compared to the mice immunized with WT-RBD only in Fig. 3B (IgG ~5.5, IgG1 ~5.6 and IgG2a ~5.5, respectively). Therefore, our data indicated singleton modification (S663V) could ameliorated the impact of pre-existing immunity and the sero-positive subjects may have chance to receive S663V-based vaccination by IM administration.

3.8. *Singleton modified vectors had good storage stability*

Higher storage temperatures will greatly enhance vaccine distribution and availability. Therefore, we compared the transducing efficiency of vectors both *in vivo* and *in vitro* after storage for intended time at 2−8 °C. As expected, we observed liquid formulation of S663V vector and WT vector showed no significant loss of transduction activity *in vitro* (Fig. 7A−C) and *in vivo* (Fig. 7D) after the storage for more than 1 month at 2−8 °C.

3.9. *AAV-based vaccines showed a good safety profile*

Although AAV vectors were recognized as the safest tools for *in vivo* gene therapy and AAV-based gene therapy medicines such as Glybera, Luxturna and Zolgensma have been approved by EMA or FDA, the safety profile of AAV-based vaccines still needs further investigation to reduce unpredictable risks. Accordingly, the H&E stain analysis of the sections of hearts, livers, spleens, lungs, kidneys and injected gastrocnemius muscles indicated that, except for mild myositis and inflammatory infiltration of adipocytes at the injected site, there were no abnormal pathological changes such as necrosis, edema, degeneration and inflammatory cell infiltration in all groups (Supporting Information Figs. S7A and S7B). Moreover, we collected the blood of immunized mice to analyze the blood biochemical indexes. The data showed that the detected values of all group were within the normal reference range (Supporting Information Fig. S8). Collectively, our preliminary data demonstrate that AAV-based vaccines have a good safety profile.

4. Discussion

The development of AAV-based vaccines generally is limited by its poor capability to induce a robust transgene-specific cellular immune response[17,46,47]. Here, a CASE strategy was developed to overcome this limitation and generate a strong and balanced humoral/cellular immune response by optimizing the antigen structure design and maximizing the DC transduction efficiency with capsid engineering.

We found that one-dose S663V-RBD vaccine could generate the best immune effect among all groups in our study, and a single dose of S663V-RBD or WT-RBD could induce a more rapid, robust and lasting RBD-specific immune response than BBIBP-CorV (Fig. 3−5). Especially, the RBD-specific IgG titer induced by S663V-RBD was significantly higher than that of some commercially available mRNA and subunit vaccines 14 days after first vaccination[7,8,10], which indicates S663V-RBD can provide protective immunity more quickly than these licensed vaccines. Overall, WT-RBD showed slightly better immunogenicity than BBIBP-CorV and maintained a stable high level of the RBD-specific binding antibody and PNAb, suggesting that the AAV6 vector has the potential to be developed as a vaccine and provide long-lasting protection by only modifying the expression cassette. In addition, considering the effectiveness against infection of two typical mRNA vaccines (mRNA-1273 and BNT162b2) declined from nearly 90% to about 50% just 6 months after full vaccination[2], we further investigated the antigen expression kinetics *via* reporter gene luciferase. We found that antigen-specific antibody could keep high level more than 4 months and intramuscular administration of transgene could stably express for more than 270 days (Fig. 2F and Fig. S5), which coincide with extensive preclinical and clinical research that the transgene of AAV could stably express for several months even years[48,49]. Meanwhile, S663V modification could enhance the transduction efficiency of both muscle cells and BMDCs (Fig. 2F and Fig. S1), which means S663V-RBD could more effectively produce antigen and activate subsequent immune responses *via* DCs. Previous studies confirmed a two-dose schedule of 2 μg BBIBP-CorV on Days 0 and 21 was sufficient to provide superior protection in mice and nonhuman primates and induce high levels of seroconversion rates and neutralization antibody titers in human[40,50]. Moreover, BBIBP-CorV demonstrated its good protective effect against SARS-CoV-2 variants such as B.1.351 (Beta) and B.1.617.2 (Delta)[51]. Therefore, our results indicate the S663V-RBD may provide a superior protective effect against SARS-CoV-2 and its variants.

For viral vector-based products for *in vivo* gene therapy, pre-existing anti-vector immune responses and critical storage conditions are two common but crucial issues. The former plagues the therapeutic effect, and the latter restricts the accessibility of users. Therefore, how to circumvent pre-existing antibodies and even reduce anti-capsid immune responses should be fully considered. In our hypothesis, local intramuscular injection will reduce viral vectors exposure to pre-existing antibodies in the circulatory system. Our data support that local intramuscular injection with modified vectors could more effectively abate the impact of pre-existing immunity than wild type vector (Fig. 6). On the other hand, according to the document *WHO Target Product Profiles for COVID-19 Vaccines*[52], product storage stability should demonstrate at least 2-week stability at 2−8 °C, and higher storage temperatures and higher thermostability are thus strongly preferred. One recent

Please cite this article as: Wu Fuhua et al., Single-shot AAV-vectored vaccine against SARS-CoV-2 with fast and long-lasting immunity, Acta Pharmaceutica Sinica B, https://doi.org/10.1016/j.apsb.2022.07.004

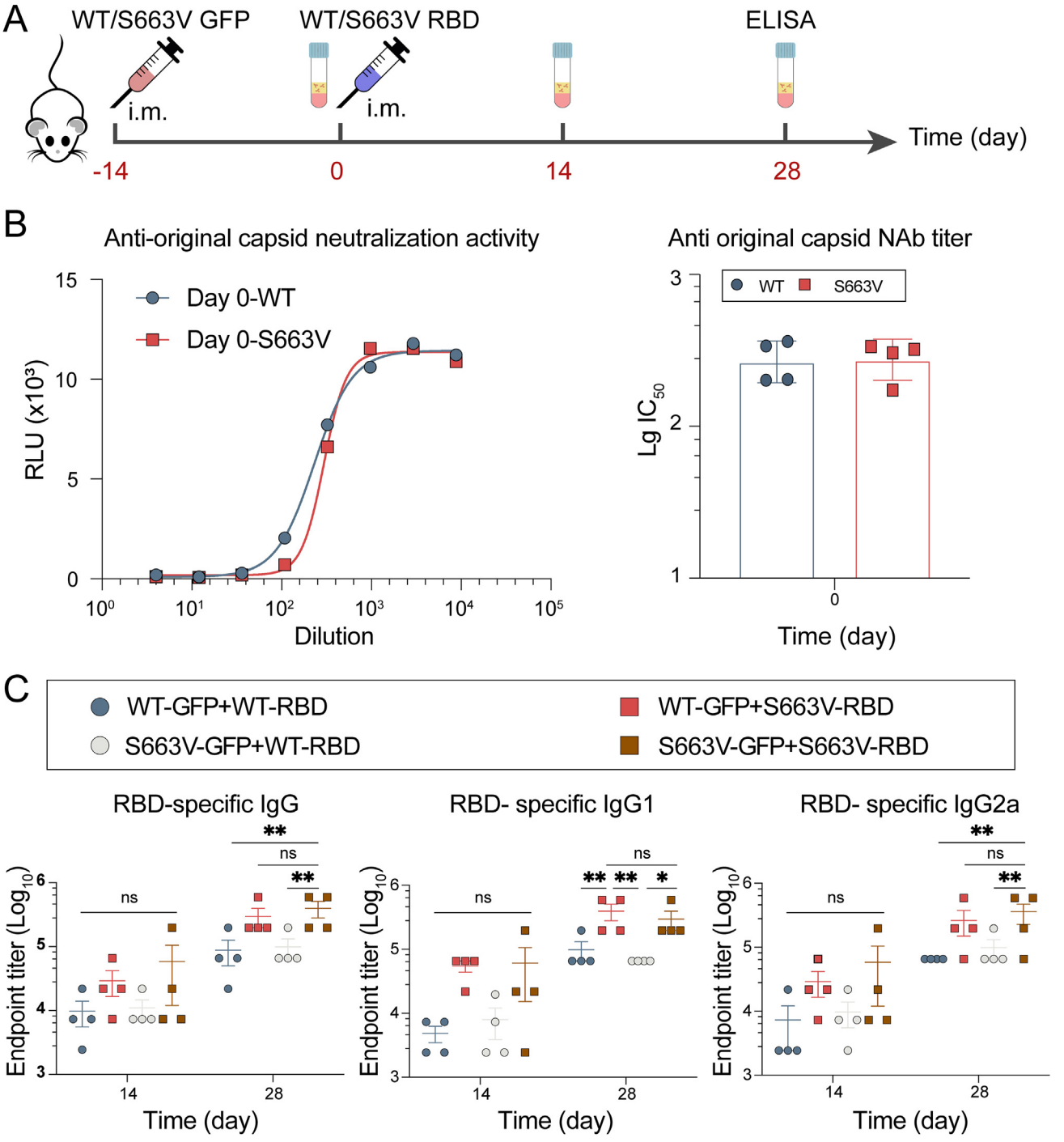

Figure 6 Intramuscular administration of singleton modification AAV overcomes pre-existing immunity. (A) The scheme of experiments. Mice were inoculated with 5×10^{10} VG of WT-GFP or S663V-GFP at same site 14 days before vaccination with 1×10^{11} VG of WT-RBD or S663V-RBD, $n = 4$. (B) The activity and level of neutralization antibody against wild type AAV6 capsid. (C) The endpoint titer of IgG, IgG1 and IgG2a under pre-existing NAbs against vector. Data are presented as mean ± SEM. Statistical significance was determined by two−way ANOVA with Tukey's multiple comparisons test (C). *$P < 0.05$ and **$P < 0.01$.

study indicated an AAVrh32.33-based vaccine can maintain vitality for more than 12 weeks at 4 °C[53]. Another previous study demonstrated that liquid AAV2 formulation was stable after 150 days of storage at both 25 and 4 °C, with only 10% loss of the original titer[54]. By applying differential scanning fluorimetry to determine the melting temperature (T_m) of AAV serotypes, the researchers found AAV6 had higher Tm than AAV2, AAV3, AAV4, AAV7, AAV8, AAV9 and AAVrh.10, which indirectly demonstrate AAV6 vectors may have better capsid thermostability[55]. Our results support that the appropriate liquid preparation can maintain the potency of WT and S663V vector without ultra-low temperature storage (Fig. 7).

Please cite this article as: Wu Fuhua et al., Single-shot AAV-vectored vaccine against SARS-CoV-2 with fast and long-lasting immunity, Acta Pharmaceutica Sinica B, https://doi.org/10.1016/j.apsb.2022.07.004

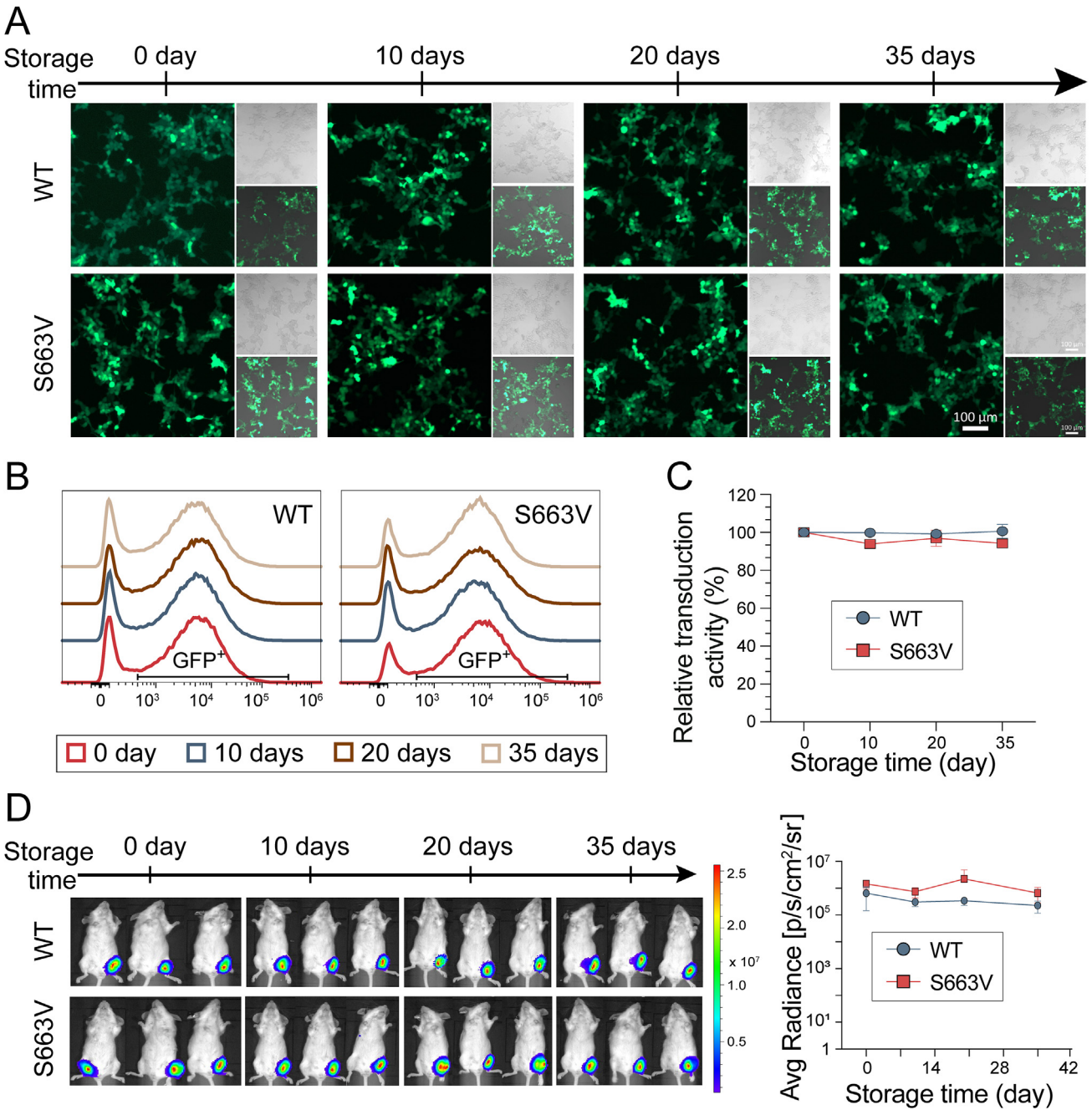

Figure 7 The storage stability of AAV6-based vaccines. The changes of transduction efficiency after storage for intended time at 2−8 °C. In vitro assay, HEK293T cells were infected (MOI 20,000) with WT-GFP or S663V-GFP. (A) After 48 h, images were collected by confocal microscope. (B), (C) Transduction efficiency changes were analyzed by FACS, and this experiment was repeated three times independently. (D) The changes of transduction efficiency *in vivo*. BALB/c female mice (6−8 weeks old) were injected intramuscularly (i.m.) with 1×10^9 VG of WT-Luc or S663V-Luc, and the transgene expression were detected after 7 days, $n = 3$. scale bars equal 100 μm.

At last but not least, a recent study demonstrated that AAV6-based mutant could steadily express transgene at a high level in sheep by intramuscular injection[56]. Another research showed that AAV6 can efficiently infect the muscle tissue adjacent to the injection site through subcutaneous injection and induce detectable T cell responses against transgene[57]. Moreover, an analysis of 149 AAV-based gene therapy trials from 2003 to 2019 demonstrated that intramuscular administration resulted in the lowest treatment-emergent serious adverse events[58]. Clinically, AAV6-based therapies administered by intravenous route (ClinicalTrials.gov) is still well tolerated, and a dose ranging from 1.5×10^{13} to 1×10^{14} VG/kg is safe on the corresponding animal models[59–61]. Through this work, we intramuscularly injected no more than 1×10^{11} VG AAV6 per mouse (about 5×10^{12} VG/kg). These data energetically support our assumption that AAV6-based vaccines hold the potential for clinical application. We also investigated the tissue morphology and inflammatory response of the main organs and injection sites, as well as the main blood biochemical indicators.

Please cite this article as: Wu Fuhua et al., Single-shot AAV-vectored vaccine against SARS-CoV-2 with fast and long-lasting immunity, Acta Pharmaceutica Sinica B, https://doi.org/10.1016/j.apsb.2022.07.004

These preliminary data indicate our AAV-based vaccine was safe within the trial cycle in mice. In addition, extensive preclinical and clinical studies proved that there are no signs of toxicity after transgene expression for years[62,63]. However, considering long-term antigen expression and its immune stimulation, we still need to carefully evaluate its benefits and risks within a longer period range.

5. Conclusions

In summary, we designed AAV-based vaccines with excellent reactogenicity by utilizing CASE strategy. Single dose S663V-RBD vaccine can generate significant wild type and variants pseudovirus neutralizing effect and superior RBD-specific cellular immune response, which indicate it would provide an endurable and effective protection in the face of the global epidemic. Considering that the evolution from viruses to mammals are conserved, CASE strategy may hold a broad application prospect to cease other infectious disease.

Acknowledgements

This work was supported by the National Natural Science Foundation of China, China (Grant Nos. 81925036 and 81872814), the Key Research and Development Program of Science and Technology Department of Sichuan Province, China (Grant No. 2020YFS0570), 111 project, China (Grant No. B18035), and the Fundamental Research Funds for the Central Universities, China. The author would like to thank China National Pharmaceutical Group Co., Ltd. (Sinopharm) for providing the licensed inactivated vaccine (BBIBP-CorV) in this study.

Author contributions

Fuhua Wu, Shuang Luo and Xun Sun designed the study and data analysis. Yongshun Zhang, Yangsen Ou, Zhaofei Guo, Chunting He, Shuting Bai, Penghui He, Min Jiang and Xiaoyan Chen assisted with the collection of the *in vivo* sample, fluorescence activating cell sorter assays and other technical support. Guangsheng Du edited language. Hairui Wang drew illustrations. Guangsheng Du, Hairui Wang, Xun Sun, Fuhua Wu and Shuang Luo contributed to the preparation of the manuscript. All authors critically reviewed and approved the final version.

Conflicts of interest

The authors have no conflicts of interest to declare.

Appendix A. Supporting information

Supporting data to this article can be found online at https://doi.org/10.1016/j.apsb.2022.07.004.

References

1. WHO Coronavirus (COVID-19) Dashboard. Availabe from: https://covid19.who.int/.
2. Cohn BA, Cirillo PM, Murphy CC, Krigbaum NY, Wallace AW. SARS-CoV-2 vaccine protection and deaths among US veterans during 2021. *Science* 2021;**375**:331−6.
3. Focosi D, Tuccori M, Baj A, Maggi F. SARS-CoV-2 Variants: a synopsis of *in vitro* efficacy data of convalescent plasma, currently marketed vaccines, and monoclonal antibodies. *Viruses* 2021;**13**:1211.
4. Garcia-Beltran WF, Lam EC, St Denis K, Nitido AD, Garcia ZH, Hauser BM, et al. Multiple SARS-CoV-2 variants escape neutralization by vaccine-induced humoral immunity. *Cell* 2021;**184**:2372−83. e9.
5. Israel A, Merzon E, Schäffer AA, Shenhar Y, Green I, Golan-Cohen A, et al. Elapsed time since BNT162b2 vaccine and risk of SARS-CoV-2 infection: test negative design study. *BMJ* 2021;**375**:e067873.
6. Vogel AB, Kanevsky I, Ye C, Swanson KA, Sahin U. Immunogenic BNT162b vaccines protect rhesus macaques from SARS-CoV-2. *Nature* 2021:1−10.
7. Corbett KS, Edwards DK, Leist SR, Abiona OM, Boyoglu-Barnum S, Gillespie RA, et al. SARS-CoV-2 mRNA vaccine design enabled by prototype pathogen preparedness. *Nature* 2020;**586**:567−71.
8. Dai L, Zheng T, Xu K, Han Y, Xu L, Huang E, et al. A universal design of betacoronavirus vaccines against COVID-19, MERS, and SARS. *Cell* 2020;**182**:722−33. e11.
9. Liang JG, Su D, Song TZ, Zeng Y, Liang P. S-Trimer, a COVID-19 subunit vaccine candidate, induces protective immunity in nonhuman primates. *Nat Commun* 2021;**12**:1346.
10. Sun S, Cai Y, Song T-Z, Pu Y, Cheng L, Xu H, et al. Interferon-armed RBD dimer enhances the immunogenicity of RBD for sterilizing immunity against SARS-CoV-2. *Cell Res* 2021;**31**:1011−23.
11. Tian JH, Patel N, Haupt R, Zhou H, Smith G. SARS-CoV-2 spike glycoprotein vaccine candidate NVX-CoV2373 immunogenicity in baboons and protection in mice. *Nat Commun* 2021;**12**:372.
12. Boonstra A. Flexibility of mouse classical and plasmacytoid-derived dendritic cells in directing T helper type 1 and 2 cell development. *J Exp Med* 2003;**197**:101−9.
13. Pandya M, Britt K, Hoffman B, Ling C, Aslanidi GV. Reprogramming immune response with capsid-optimized AAV6 vectors for immunotherapy of cancer. *J Immunother* 2015;**38**:292−8.
14. Manno CS, Arruda VR, Pierce GF, Glader B, Ragni M, Rasko J, et al. Successful transduction of liver in hemophilia by AAV-Factor IX and limitations imposed by the host immune response. *Nat Med* 2006;**12**:342−7.
15. Chengwen Li, Hirsch Matt, DiPrimio Nina, et al. Cytotoxic-T-lymphocyte-mediated elimination of target cells transduced with engineered adeno-associated virus type 2 vector in vivo. *J Virol* 2009;**83**:6817−24.
16. Greig JA, Calcedo R, Grant RL, Hui P, Wilson JM. Intramuscular administration of AAV overcomes pre-existing neutralizing antibodies in rhesus macaques. *Vaccine* 2016;**34**:6323−9.
17. Brockstedt DG, Podsakoff GM, Fong L, Kurtzman G, Mueller-Ruchholtz W, Engleman EG. Induction of immunity to antigens expressed by recombinant adeno-associated virus depends on the route of administration. *Clin Immunol* 1999;**92**:67−75.
18. Pandya J, Ortiz L, Ling C, Rivers AE, Aslanidi G. Rationally designed capsid and transgene cassette of AAV6 vectors for dendritic cell-based cancer immunotherapy. *Immunol Cell Biol* 2013;**92**:116−23.
19. Van L, Domm JM, Rindler TN, Frost KL, Sorensen DL, Medina SJ, et al. A novel triple-mutant AAV6 capsid induces rapid and potent transgene expression in the muscle and respiratory tract of mice. *Mol Ther Methods Clin Dev* 2018;**9**:323−9.
20. Zhong L, Li B, Mah CS, Govindasamy L, Agbandje-McKenna M, Cooper M, et al. Next generation of adeno-associated virus 2 vectors: point mutations in tyrosines lead to high-efficiency transduction at lower doses. *Proc Natl Acad Sci U S A* 2008;**105**:7827.
21. Li C, Diprimio N, Bowles DE, Hirsch ML, Monahan PE, Asokan A, et al. Single amino acid modification of adeno-associated virus capsid changes transduction and humoral immune profiles. *J Virol* 2012;**86**:7752−9.
22. Li C, He Y, Nicolson S, Hirsch M, Weinberg MS, Zhang P, et al. Adeno-associated virus capsid antigen presentation is dependent on endosomal escape. *J Clin Invest* 2013;**123**:1390−401.
23. Wrapp D, Wang N, Corbett KS, Goldsmith JA, Hsieh C-L, Abiona O, et al. Cryo-EM structure of the 2019-nCoV spike in the prefusion conformation. *Science* 2020;**367**:1260−3.

24. Rey FA, Stiasny K, Vaney M-C, Dellarole M, Heinz FX. The bright and the dark side of human antibody responses to flaviviruses: lessons for vaccine design. *EMBO Rep* 2018;**19**:206−24.
25. Liu Y, Soh WT, Kishikawa J-I, Hirose M, Nakayama EE, Li S, et al. An infectivity-enhancing site on the SARS-CoV-2 spike protein targeted by antibodies. *Cell* 2021;**184**:3452−66. e18.
26. Tao Y, Strelkov SV, Mesyanzhinov VV, Rossmann MG. Structure of bacteriophage T4 fibritin: a segmented coiled coil and the role of the C-terminal domain. *Structure* 1997;**5**:789−98.
27. Shanmugam A, Rajoria S, George AL, Mittelman A, Suriano R, Tiwari RK. Synthetic toll like receptor-4 (TLR-4) agonist peptides as a novel class of adjuvants. *PLoS One* 2012;**7**:e30839.
28. Wu S, Zhong G, Zhang J, Shuai L, Zhang Z, Wen Z, et al. A single dose of an adenovirus-vectored vaccine provides protection against SARS-CoV-2 challenge. *Nat Commun* 2020;**11**:4081.
29. Khoury DS, Cromer D, Reynaldi A, Schlub TE, Davenport MP. Neutralizing antibody levels are highly predictive of immune protection from symptomatic SARS-CoV-2 infection. *Nat Med* 2021;**27**:1205−11.
30. Turner JS, O'Halloran JA, Kalaidina E, Kim W, Schmitz AJ, Zhou JQ, et al. SARS-CoV-2 mRNA vaccines induce persistent human germinal centre responses. *Nature* 2021;**596**:109−13.
31. Du X, Hou Y, Huang J, Pang Y, Ruan C, Wu W, et al. Cytosolic delivery of the immunological adjuvant Poly I:C and cytotoxic drug crystals via a carrier-free strategy significantly amplifies immune response. *Acta Pharm Sin B* 2021;**11**:3272−85.
32. Zhong X, Zhang Y, Tan L, Zheng T, Hou Y, Hong X, et al. An aluminum adjuvant-integrated nano-MOF as antigen delivery system to induce strong humoral and cellular immune responses. *J Control Release* 2019;**300**:81−92.
33. Li J, Lu J, Guo H, Zhou J, Wang S, Jiang K, et al. A pentapeptide enabled AL3810 liposome-based glioma-targeted therapy with immune opsonic effect attenuated. *Acta Pharm Sin B* 2021;**11**:283−99.
34. Zhang Y, Jiang M, Du G, Zhong X, He C, Qin M, et al. An antigen self-assembled and dendritic cell-targeted nanovaccine for enhanced immunity against cancer. *Acta Pharm Sin B* 2022. https://doi.org/10.1016/j.apsb.2022.03.017. Available from:.
35. Guo Z, Zhu Y, Du G, Qin M, He C, He P, et al. Rapid development of a subunit nano-vaccine against drug-resistant Pseudomonas aeruginosa with effective cross-protection. *Nano Today* 2022;**43**:101398.
36. Lin J, Calcedo R, Vandenberghe LH, Bell P, Somanathan S, Wilson JM. A new genetic vaccine platform based on an adeno-associated virus isolated from a rhesus macaque. *J Virol* 2009;**83**:12738−50.
37. Liao G, Fan X, Lau H, Liu Z, Li C, Xu Z, et al. Single-shot rAAV5-based vaccine provides long-term protective immunity against sars-cov-2 and its variants. *bioRxiv* 2021. 2021.08.23.456471. Available from: https://www.biorxiv.org/content/10.1101/2021.08.23.456471v1.full.pdf.
38. Grimm D, Lee JS, Wang L, Desai T, Akache B, Storm TA, et al. In vitro and *in vivo* gene therapy vector evolution via multispecies interbreeding and retargeting of adeno-associated viruses. *J Virol* 2008;**82**:5887−911.
39. Ussher JE, Taylor JA. Optimized transduction of human monocyte-derived dendritic cells by recombinant adeno-associated virus serotype 6. *Hum Gene Ther* 2010;**21**:1675−86.
40. Wang H, Zhang Y, Huang B, Deng W, Yang X. Development of an inactivated vaccine candidate, BBIBP-CorV, with potent protection against SARS-CoV-2. *Cell* 2020;**182**:713−21. e9.
41. Feng S, Phillips DJ, White T, Sayal H, Aley PK, Bibi S, et al. Correlates of protection against symptomatic and asymptomatic SARS-CoV-2 infection. *Nat Med* 2021;**27**:2032−40.
42. Kimura I, Kosugi Y, Wu J, Zahradnik J, Yamasoba D, Butlertanaka EP, et al. The SARS-CoV-2 Lambda variant exhibits enhanced infectivity and immune resistance. *Cell Rep* 2022;**38**:110218.
43. Mlcochova P, Kemp SA, Dhar MS, Papa G, Meng B, Ferreira IA, TM, et al. SARS-CoV-2 B.1.617.2 Delta variant replication and immune evasion. *Nature* 2021;**599**:114−9.
44. Lederer K, Castao D, Atria DG, Oguin TH, Locci M. SARS-CoV-2 mRNA vaccines foster potent antigen-specific germinal center responses associated with neutralizing antibody generation. *Immunity* 2020;**53**:1281−95. e5.
45. Limberis M,P, Wilson J,M. Adeno-associated virus serotype 9 vectors transduce murine alveolar and nasal epithelia and can be readministered. *Proc Natl Acad Sci U S A* 2006;**103**:12993−8.
46. Demminger DE, Walz L, Dietert K, Hoffmann H, Planz O, Gruber AD, et al. Adeno-associated virus-vectored influenza vaccine elicits neutralizing and Fcγ receptor-activating antibodies. *EMBO Mol Med* 2020;**12**. e10938-e.
47. Hensel JA, Khattar V, Ashton R, Ponnazhagan S. Recombinant AAV-CEA tumor vaccine in combination with an immune adjuvant breaks tolerance and provides protective immunity. *Mol Ther Oncolytics* 2018;**12**:41−8.
48. Pasi KJ, Rangarajan S, Mitchell N, Lester W, Symington E, Madan B, et al. Multiyear follow-up of AAV5-hFVIII-SQ gene therapy for hemophilia A. *N Engl J Med* 2020;**382**:29−40.
49. George LA, Ragni MV, Rasko J, Raffini LJ, High KA. Long-term follow-up of the first in human intravascular delivery of AAV for gene transfer: AAV2-hFIX16 for severe hemophilia B. *Mol Ther* 2020;**28**:2073−82.
50. Xia S, Zhang Y, Wang Y, Wang H, Yang X. Safety and immunogenicity of an inactivated SARS-CoV-2 vaccine, BBIBP-CorV: a randomised, double-blind, placebo-controlled, phase 1/2 trial. *Lancet Infect Dis* 2020;**21**:39−51.
51. Jeewandara C, Aberathna IS, Pushpakumara PD, Kamaladasa A, Guruge D, Wijesinghe A, et al. Persistence of immune responses to the Sinopharm/BBIBP-CorV vaccine. *Immun Inflammation Dis* 2022;**10**:e621.
52. WHO target product profiles for COVID-19 vaccines. Available from: https://cdn.who.int/media/docs/default-source/blue-print/tpp-6apr-2022-final.pdf?sfvrsn=4f8cede5_3&download=true.
53. Zabaleta N, Dai W, Bhatt U, Hérate C, Maisonnasse P, Chichester JA, et al. An AAV-based, room-temperature-stable, single-dose COVID-19 vaccine provides durable immunogenicity and protection in non-human primates. *Cell Host Microbe* 2021;**29**:1437−53. e8.
54. Croyle MA, Cheng X, Wilson JM. Development of formulations that enhance physical stability of viral vectors for gene therapy. *Gene Ther* 2001;**8**:1281.
55. Antonette Bennett, Saajan Patel, Mario Mietzsch, et al. Thermal stability as a determinant of AAV serotype identity. *Mol Ther Methods Clin Dev* 2017;**6**:171−82.
56. Rghei AD, Van Lieshout LP, McLeod BM, Pei Y, Lopes JA, Zielinska N, et al. Safety and tolerability of the adeno-associated virus vector, AAV6.2FF, expressing a monoclonal antibody in murine and ovine animal models. *Biomedicines* 2021;**9**:1186.
57. Stone D, Kenkel EJ, Loprieno MA, Tanaka M, Jerome KR. Gene transfer in adeno-associated virus seropositive rhesus macaques following rapamycin treatment and subcutaneous delivery of AAV6, but not retargeted AAV6 vectors. *Hum Gene Ther* 2020;**32**:96−112.
58. Kuzmin DA, Shutova MV, Johnston NR, Smith OP, Johnstone EC. The clinical landscape for AAV gene therapies. *Nat Rev Drug Discov* 2021;**20**:173−4.
59. Grimm D, Zhou S, Nakai H, Thomas CE, Storm TA, Fuess S, et al. Preclinical *in vivo* evaluation of pseudotyped adeno-associated virus vectors for liver gene therapy. *Blood* 2003;**102**:2412−9.
60. Jiang H, Lillicrap D, Patarroyo-White S, Liu T, Qian X, Scallan CD, et al. Multiyear therapeutic benefit of AAV serotypes 2, 6, and 8 delivering factor VIII to hemophilia A mice and dogs. *Blood* 2006;**108**:107−15.
61. Yasuda M, Huston MW, Pagant S, Gan L, St Martin S, Sproul S, et al. AAV2/6 gene therapy in a murine model of fabry disease results in supraphysiological enzyme activity and effective substrate reduction. *Mol Ther Methods Clin Dev* 2020;**18**:607−19.
62. Le Meur G, Lebranchu P, Billaud F, Adjali O, Schmitt S, Bézieau S, et al. Safety and long-term efficacy of AAV4 gene therapy in patients with RPE65 leber congenital amaurosis. *Mol Ther* 2018;**26**:256−68.
63. Sabatino DE, Lange AM, Altynova ES, Sarkar R, Zhou S, Merricks EP, et al. Efficacy and safety of long-term prophylaxis in severe hemophilia a dogs following liver gene therapy using AAV vectors. *Mol Ther* 2011;**19**:442−9.

Please cite this article as: Wu Fuhua et al., Single-shot AAV-vectored vaccine against SARS-CoV-2 with fast and long-lasting immunity, Acta Pharmaceutica Sinica B, https://doi.org/10.1016/j.apsb.2022.07.004